5358 *Biochemistry* **2010,** *49,* 5358–5365
DOI: 10.1021/bi1003958

BIOCHEMISTRY
including biophysical chemistry & molecular biology
Article

Biochemical Properties and Biological Function of a Monofunctional Microbial Biotin Protein Ligase[†]

Kyle G. Daniels and Dorothy Beckett*

Department of Chemistry and Biochemistry, Center for Biological Structure and Organization, University of Maryland, College Park, Maryland 20742

Received March 15, 2010; Revised Manuscript Received May 14, 2010

ABSTRACT: Biotin protein ligases constitute a family of enzymes that catalyze the linkage of biotin to biotin-dependent carboxylases. In bacteria, these enzymes are functionally divided into two classes: the monofunctional enzymes that catalyze only biotin addition and the bifunctional enzymes that also bind to DNA to regulate transcription initiation. Biochemical and biophysical studies of the bifunctional *Escherichia coli* ligase suggest that several properties of the enzyme have evolved to support its additional regulatory role. Included among these properties are the order of substrate binding and linkage between the oligomeric state and ligand binding. To test this hypothesized relationship between functionality and biochemical properties in ligases, we have conducted studies of the monofunctional ligase from *Pyrococcus horikoshii*. Sedimentation equilibrium measurements to determine the effect of ligand binding on oligomerization indicate that the enzyme exists as a dimer regardless of liganded state. Measurements performed using isothermal titration calorimetry and fluorescence spectroscopy indicate that, in contrast to the bifunctional *E. coli* enzyme, substrate binding does not occur by an obligatorily ordered mechanism. Finally, thermodynamic signatures of ligand binding to the monofunctional enzyme differ significantly from those measured for the bifunctional enzyme. These results indicate a correlation between the functional complexity of biotin protein ligases and their detailed biochemical characteristics.

Biotin-dependent carboxylases in all organisms utilize biotin to mediate carboxyl group transfer reactions. An example of this class of enzyme is acetyl-CoA[1] carboxylase, which catalyzes the conversion of acetyl-CoA to malonyl-CoA, the first committed step of fatty acid biosynthesis. In its coenzyme function, biotin is covalently linked to the biotin carboxyl carrier protein, BCCP, of the carboxylase via an amide linkage between the carboxylic acid group of the valerate chain of the coenzyme and the ε-amino group of a specific lysine side chain of BCCP. The post-translational biotin modification is catalyzed by biotin protein ligases (BPLs) in the following two-step reaction:

$$\mathrm{BPL} + \mathrm{biotin} + \mathrm{ATP} \rightleftharpoons \mathrm{BPL \cdot bio\text{-}5'\text{-}AMP} + \mathrm{PP_i}$$

$$\mathrm{BPL \cdot bio\text{-}5'\text{-}AMP} + \mathrm{apocarboxylase} \rightarrow \mathrm{BPL} + \mathrm{holocarboxylase} + \mathrm{AMP}$$

in which the activated biotin, bio-5′-AMP, is first synthesized by BPL from substrates biotin and ATP and the biotin is subsequently transferred to the lysine residue of the BCCP moiety of the apocarboxylase (*1*).

Two classes of BPLs have been identified in microorganisms (*2*, *3*). Enzymes in the first class, of which the *Pyrococcus horikoshii* enzyme is a member, catalyze only post-translational biotin addition. The second class includes the well-characterized *Escherichia coli* enzyme, which functions not only as a post-translational modification enzyme but also as a transcriptional repressor (Figure 1) (*4*, *5*). As a repressor, the *E. coli* enzyme prevents transcription initiation at the two promoters of the biotin biosynthetic operon (*4*, *5*). Thus, the *E. coli* enzyme both funnels biotin into metabolism and regulates expression of the genes that encode biotin biosynthetic enzymes. Both classes of BPLs are found throughout the eubacterial and archael kingdoms (*2*, *3*).

The primary sequences and high-resolution structures of representatives of the two classes of microbial biotin protein ligases indicate similarities as well as striking differences. All microbial biotin holoenzyme ligase sequences are characterized by a homologous region of approximately 250 amino acid residues, which is required for catalytic function. Additionally, the bifunctional ligases possess an N-terminal segment that encodes a winged helix−turn−helix DNA binding domain (*2*). High-resolution three-dimensional structures of representatives of both classes of ligases have been obtained using X-ray crystallography (*6*−*10*). Comparison of the structures of the *E. coli* and *P. horikoshii* enzyme monomers reveals, with the exception of the DNA binding domain at the N-terminus of the *E. coli* enzyme, great similarity (Figure 2). However, the structures diverge at the quaternary level. Structures of the unliganded proteins indicate that while the *E. coli* enzyme is a monomer, the *P. horikoshii* enzyme self-associates via extension of the central β-sheet at its N-terminus forming an elongated dimer. Liganded forms of the *P. horikoshii* enzyme show this same dimeric structure. By contrast, the *E. coli* enzyme is dimeric only in structures in which

[†]Supported by National Institutes of Health Grants R01-GM46511 and S10-RR15899 to D.B. and a Howard Hughes Medical Institute Undergraduate Research Fellowship to K.G.D.

*To whom correspondence should be addressed. E-mail: dbeckett@umd.edu. Telephone: (301) 405-1812. Fax: (301) 314-9121.

[1]Abbreviations: *Ph*BPL, *Pyrococcus horikoshii* biotin protein ligase; ITC, isothermal titration calorimetry; CoA, coenzyme A; BCCP, biotin carboxyl carrier protein; Tris, tris(hydroxymethyl)aminomethane; IPTG, isopropyl β-D-thiogalactoside.

 Published on Web 05/25/2010

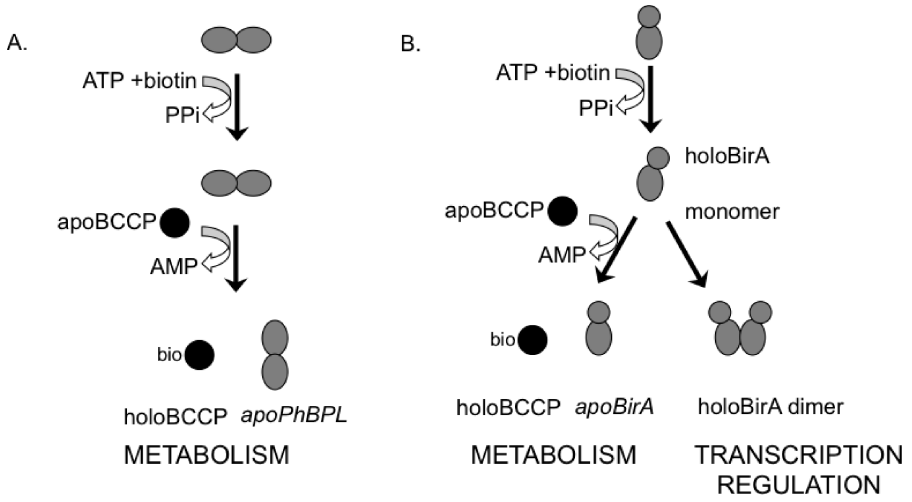

FIGURE 1: (A) Monofunctional *Ph*BPL biotinylates the biotin carboxyl carrier protein (BCCP) subunit of biotin-dependent carboxylases. (B) Bifunctional BirA can biotinylate BCCP or form a homodimer that acts as a transcriptional repressor of biotin biosynthetic genes.

FIGURE 2: (A) *P. horikoshii* BPL monomer. (B) BirA monomer. *P. horikoshii* BPL homodimer. (D) BirA homodimer. Models were constructed in MolMol (*28*) with Protein Data Bank entries 1WPY (A and C) and 2EWN (B and D). The *Ph*BPL monomer in panel A and the BirA monomer in panel B were each obtained by deletion of the second monomer from their respective dimer models.

it is bound to biotin or to an analogue of the intermediate in the reaction, bio-5′-AMP (*6*−*8*). Moreover, the surface utilized for dimerization is completely distinct (Figure 2) from that employed by the *P. horikoshii* enzyme. The *E. coli* holoBirA homodimer is the active species in site-specific DNA binding that is associated with its transcription repression function (*11*, *12*).

Biochemical studies of the *E. coli* biotin protein ligase suggest that the detailed mechanistic properties of the enzyme have evolved to support its bifunctionality. First, kinetic measurements of bio-5′-AMP synthesis from biotin and ATP indicate an obligatorily ordered mechanism for substrate binding, with biotin binding first followed by ATP (*13*). This mechanism is supported by structural data that indicate that the ATP binding site is formed as a consequence of biotin-induced folding of specific loop segments in BirA (*7*). In addition, formation of the adenylate from ATP and biotin is a prerequisite for stable BirA dimerization in solution. Sedimentation equilibrium measurements indicate that while apoBirA and BirA-biotin dimerize very weakly, the adenylate-bound protein dimerizes in the micromolar protein concentration range (*14*). Because BirA homodimerization is required for DNA binding, the thermodynamic coupling of self-association to adenylate synthesis combined with the ordered mechanism of biotin and ATP binding renders DNA binding itself subject to regulation by intracellular biotin concentration (*12*). Finally, a single surface of the *E. coli* enzyme is used for both homodimerization with another holoBirA monomer and heterodimerization with apoBCCP (*15*−*17*). This feature has consequences for the regulation of switching between enzymatic and site-specific DNA binding functions.

The pathway of evolution of bifunctionality in biotin holoenzyme ligases is not known. However, it is likely that the coding sequence for the DNA binding domain was linked to that for the catalytic function through a gene fusion event. Biochemical and biophysical studies of the *E. coli* enzyme indicate these two structural elements are functionally coupled through formation of the active adenylate-bound enzyme, holoBirA, which both catalyzes biotin transfer and binds sequence-specifically to DNA to repress transcription initiation (*18*). The obligatorily ordered mechanism of biotin binding followed by ATP renders formation of the activated species exquisitely sensitive to biotin concentration (*13*). We hypothesize that the monofunctional enzymes, which only transfer biotin to apocarboxylases and play no regulatory role, do not employ this ordered mechanism.

In this work, the relationship between mechanistic properties and functionality in microbial biotin protein ligases is investigated in the monofunctional *P. horikoshii* ligase. Measurements of the assembly state of the enzyme in the absence and presence of ligand indicate that, regardless of ligation state, it is dimeric in solution. Measurements of biotin and ATP binding using combined isothermal titration calorimetry and fluorescence spectroscopy indicate that the enzyme can bind each substrate in a manner independent of the second and that in binding the individual substrates no interaction between the two sites in the dimer exists. Furthermore, measurements of substrate binding, ATP or biotin, in the presence of saturating concentrations of the second substrate indicate no linkage in binding of the two substrates to the active site in each monomer. The combined results indicate that in mono- and bifunctional biotin protein ligases the mechanistic properties of the enzymes correlate with the complexity of their functional properties.

MATERIALS AND METHODS

Chemicals and Biochemicals. All chemicals used in buffer preparation were at least reagent grade. The *d*-biotin, adenosine 5′-triphosphate, and α,β-methyleneadenosine 5′-triphosphate were purchased from Sigma Aldrich. Solutions of ATP and the ATP analogue were prepared by dissolving the dried powder in H_2O followed by adjustment of the pH to 7.5. The resulting solutions were divided into 1 mL aliquots that were stored at −70 °C. The nucleotide concentration was determined by UV absorption spectroscopy using an extinction coefficient of 15900 M^{-1} cm^{-1} at 259 nm. Biotin solutions were prepared by dissolving the desired amount of dried powder in standard buffer (10 mM Tris-HCl, 500 mM KCl, and 2.5 mM $MgCl_2$) that had not yet had its pH adjusted. The pH of the resulting solution was adjusted to 7.5, and the solution was brought to its final volume in a volumetric flask. After the solution had been passed through a 0.22 μm filter, it was divided into 1.0 mL aliquots that were stored at −70 °C. The bio-5′-AMP was synthesized and purified as previously described (*1*, *11*).

P. horikoshii Biotin Protein Ligase Purification. The plasmid encoding the *P. horikoshii* biotin protein ligase, which was obtained from RIKEN, is a derivative of pET-11a in which expression of the *Ph*BPL coding sequence is under the control of the T7 promoter. The plasmid was transformed into *E. coli* strain BL21-λDE3 RIL. All cell growth was performed in LB medium supplemented with 100 μg/mL ampicillin. Starter cultures were produced by dilution of 5 mL of an overnight culture into 50 mL of LB/ampicillin and grown while being shaken at 37 °C. One liter of medium was inoculated with 20 mL of starter culture and incubated at 37 °C until the OD_{600} reached a value of 0.9, at which time a fresh solution of IPTG was added to the culture to a final concentration of 75 μg/mL and cell growth was continued for an additional 4 h. All manipulations following cell growth, with the exception of a single heating step, were performed at 4 °C. The cells were harvested by centrifugation at 4 °C and 6000 rpm for 30 min, resuspended in 20 mM Tris-HCl and 0.5 M NaCl (pH 8.0) at 4 °C, and lysed by sonication. After removal of cellular debris by centrifugation at 9000 rpm for 30 min, the supernatant was treated with polyethyleneimine [final concentration of 0.2% (v/v)] to remove nucleic acids. Following separation of the precipitate by centrifugation at 9000 rpm for 30 min, the resulting supernatant was heated at 91 °C for 11 min to denature contaminating proteins. The precipitated contaminating proteins were pelleted by centrifugation for 30 min at 9000 rpm, and the resulting supernatant was combined with 3 volumes of saturated ammonium sulfate and stirred gently at 4 °C overnight. The ammonium sulfate precipitate was separated from the supernatant by centrifugation at 9000 rpm for 30 min, and the resulting pellet was resuspended in 20 mL of buffer containing 50 mM Tris-HCl (pH 7.5), 50 mM KCl, and 5% (v/v) glycerol at 4 °C (SP starting buffer). After the sample had been extensively dialyzed against the same buffer, it was loaded onto a 20 mL column packed with SP-Sepharose resin (Perkin-Elmer) at a flow rate of 0.5 mL/min. The column was washed extensively with the starting buffer at the same flow rate, and the protein was eluted with a gradient from 50 to 500 mM KCl (total volume of 200 mL). Samples were analyzed by sodium dodecyl sulfate−polyacrylamide gel electrophoresis (SDS−PAGE), and those containing the pure protein were pooled and dialyzed against buffer containing 50 mM Tris-HCl, 200 mM KCl, and 5% (v/v) glycerol (pH 7.5) at 4 °C. The pure protein was stored in 1 mL aliquots in silanized 1.5 mL Eppendorf tubes at −70 °C. The protein concentration was determined spectrophotometrically using an extinction coefficient at 280 nm of 23470 M^{-1} cm^{-1} (*19*).

Analytical Ultracentrifugation. The assembly state of *Ph*BPL was determined using analytical ultracentrifugation in a Beckman-Coulter XL-I analytical ultracentrifuge. All measurements were performed using six-hole charcoal-filled Epon centerpieces (1.2 cm) equipped with sapphire windows. The protein was first dialyzed exhaustively against standard buffer [10 mM Tris-HCl (pH 7.5), 500 mM KCl, and 2.5 mM $MgCl_2$ at 20 °C] and then diluted to the appropriate concentration for centrifugation. Samples containing protein alone or protein with saturating concentrations of biotin or bio-5′-AMP were centrifuged at speeds ranging from 20000 to 24000 rpm. Scans were acquired at 280 nm (apo*Ph*BPL and biotin bound) or 295 nm (bio-5′-AMP bound) at a step size of 0.001 nm with four averages per step. The data scans were analyzed with WinNonLin (*20*) using a single-species model to obtain a reduced molecular weight, σ, from which a molecular weight was calculated using the following equation:

$$\sigma = \frac{M(1-\bar{v}\rho)\omega^2}{RT}$$

where M is the molecular weight, $\bar{v}$ is the partial specific volume of the protein calculated from the amino acid composition (SedenTerp, http://www.rasmb.bbri.org), ρ is the solvent density determined pycnometrically, ω is the angular velocity of the rotor, and R is the gas constant.

Isothermal Titration Calorimetry. Isothermal titration calorimetry was performed using a MicroCal VP-ITC instrument

(GE Healthcare). The protein was prepared for measurements by exhaustive dialysis against the appropriate buffer and then diluted into the dialysis buffer to the final desired concentration, degassed, and placed in the sample cell. Ligand was prepared by dilution of the stock into the same buffer used for the dialysis and placed in the syringe. Titrations were performed via injection of the concentrated ligand solution into the protein solution, and the mixture was stirred at a rate of 310 rpm. The protein concentration in the sample cell ranged from 2 to 4 μM, and the ligand concentration in the syringe was 20−40 μM. Binding data were analyzed using a simple 1:1 binding model using Origin (GE Healthcare).

Fluorescence Spectroscopy. All fluorescence titrations were performed using an ISS PC1 spectrofluorometer equipped with a circulating water bath to maintain a constant temperature. The excitation wavelength was 295 nm, and emission spectra were acquired from 310 to 450 nm. The excitation and emission bandpasses were each set at 8 nm. Spectra were acquired as the average of 10 iterations with a step size of 1 nm and a scan rate of 1 nm/s. Both the total intensity (corrected for buffer contribution) and the first moment of each spectrum were recorded. Titrations were performed by pipetting small aliquots of ligand into the protein in a quartz cuvette, stirring the mixture manually, and allowing the system to reach equilibrium via incubation for 2 min prior to the acquisition of spectra. Simple titrations of the *Ph*BPL with ATP, the ATP analogue, and biotin were performed as well as titrations with biotin in the presence of saturating levels of the ATP analogue and the ATP analogue in the presence of a saturating level of biotin. Data from titrations were analyzed by nonlinear least-squares analysis in Prism 4 (GraphPad) using a simple binding model to obtain the equilibrium association constant for binding and the fluorescence signal (total intensity or spectrum moment) for the ligand-free and -bound protein. The temperature dependencies of ATP and biotin binding were measured via titrations in buffer prepared at the indicated temperatures.

RESULTS

PhBPL Is Always a Dimer in Solution. Structures of several forms of the *P. horikoshii* biotin protein ligase have been determined by X-ray crystallography. These include the apo or unliganded enzyme, the enzyme bound to ADP, biotin, and bio-5′-AMP (*9*). In all of these structures, the protein is a dimer. However, the dimeric state in the crystal structure may not extend to the protein in solution at a low total concentration. The solution state assembly properties of *Ph*BPL were measured using a sedimentation equilibrium. Protein samples prepared at multiple loading concentrations were centrifuged at multiple speeds, and the data were globally analyzed using a single-species model. Results of analysis of data obtained for the unliganded protein, which has a monomer molecular mass of 26 kDa, indicate that it is well-modeled as a single species with a molecular mass of 51.2 ± 0.2 kDa (Figure 3). Measurements performed in the presence of a saturating level of biotin or bio-5′-AMP also yielded molecular masses consistent with a dimer. Thus, regardless of ligation state, *Ph*BPL is a dimer in solution.

Biotin Binding by PhBPL. Biotin binding to *Ph*BPL was monitored using steady state fluorescence emission spectroscopy. The intensity of the intrinsic protein fluorescence signal of the ligase, the sequence of which contains three tryptophan residues per monomer, is quenched by 30% upon addition of saturating concentrations of the substrate biotin (Figure 4A). Furthermore,

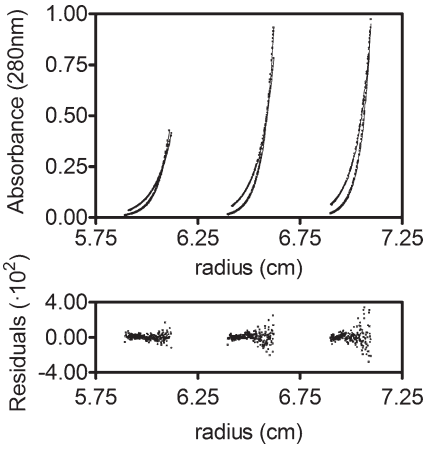

FIGURE 3: Sedimentation equilibrium concentration distributions for *Ph*BPL. Concentration profiles were obtained from samples prepared at 5.3, 10.7, and 18 μM protein monomer in standard buffer and centrifuged at 20000 (○) and 24000 rpm (□). The solid lines represent results of global nonlinear least-squares analysis of six data sets. The bottom panel indicates the residuals of the fit.

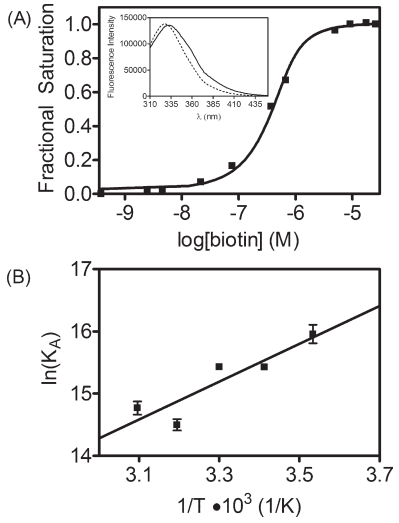

FIGURE 4: Biotin binding to *Ph*BPL. (A) Normalized binding data obtained via titration of *Ph*BPL with biotin at 20 °C. The solid line represents the best fit obtained from nonlinear least-squares analysis of the data using a single-site binding model. The inset shows the fluorescence emission spectra acquired for *Ph*BPL (—) and the *Ph*BPL·biotin complex (···). (B) van't Hoff analysis of the temperature dependence of the equilibrium association constant for the *Ph*BPL−biotin interaction obtained from titrations performed from 10 to 50 °C. The solid line represents the best fit of the data to the van't Hoff equation.

the emission maximum shifts to the blue by approximately 5 nm. These spectral changes were exploited in monitoring biotin binding. Titration of the protein with the ligand yields an isotherm that is consistent with a simple binding process (Figure 4A). Nonlinear least-squares analysis of the data using a simple binding model yields an equilibrium constant of (2.0 ± 0.1) × 10^{-7} M at 20 °C (Table 1).

The organism *P. horikoshii* was isolated from a deep sea thermal vent and grows optimally at 98 °C (*21*). Although it is technically impossible to measure biotin binding at this optimal growth temperature, titrations could be performed over a range of temperatures up to 50 °C. Results of these measurements indicate that the binding adheres to a simple mechanism over the entire temperature range and that the equilibrium dissociation

Table 1: Temperature Dependence of Biotin Binding to *Ph*BPL

temperature[a] (°C)	K_D[b] (M)	$\Delta G^{\circ c}$ (kcal/mol)
10	$(1.2 \pm 0.3) \times 10^{-7}$	-8.96 ± 0.01
20	$(2.0 \pm 0.1) \times 10^{-7}$	-8.90 ± 0.04
30	$(2.0 \pm 0.2) \times 10^{-7}$	-9.20 ± 0.05
40	$(5.1 \pm 0.8) \times 10^{-7}$	-8.93 ± 0.09
50	$(3.9 \pm 0.7) \times 10^{-7}$	-9.4 ± 0.1

[a]Measurements were performed in standard buffer [500 mM KCl, 10 mM Tris-HCl, and 2.5 mM $MgCl_2$ (pH 7.5 ± 0.2) at the indicated temperature] as described in Materials and Methods. [b]Errors correspond to the standard deviation of results obtained from at least two independent experiments. [c]The free energy, ΔG°, is related to the equilibrium constant, K_D, by the expression $\Delta G^\circ = RT \ln K_D$.

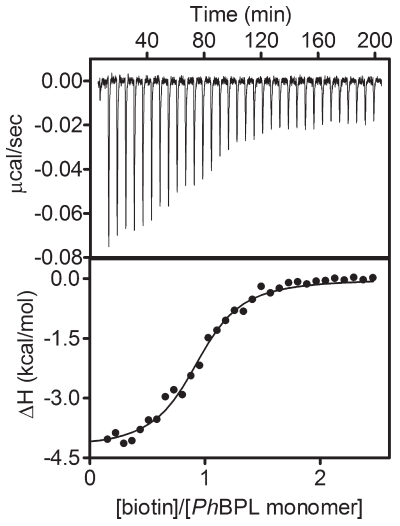

FIGURE 5: Calorimetric titration of *Ph*BPL with biotin obtained by ITC from thirty-three 9 μL injections of 40 μM ligand into a 4 μM protein solution in standard buffer at 20 °C. The solid line represents the best fit of the data to a single-site binding model.

constant increases by approximately 4-fold when the temperature is increased from 10 to 50 °C (Table 1). Analysis of the dependence of the equilibrium association constant on temperature using the van't Hoff formalism yields an enthalpy of binding of -4.4 ± 0.2 kcal/mol. Direct titrations of the enzyme with biotin performed using isothermal titration calorimetry at 20 °C confirm this binding enthalpy and yield an equilibrium association for the binding process identical to that measured by fluorescence titrations (Figure 5). Finally, measurement of the temperature dependence of binding by ITC reveals a heat capacity change of 5 ± 14 cal mol^{-1} K^{-1}, consistent with the assumption of the van't Hoff analysis that the binding enthalpy is temperature-independent (Figure 7B).

ATP Binding. Saturation of the protein with ATP results in quenching of 60% of the fluorescence signal of the protein and a blue shift of approximately 5 nm (Figure 6A). These fluorescence changes enabled titrations for the determination of the affinity and binding mode for ATP. A titration performed at 20 °C yields data that are described well by a simple binding model, and nonlinear least-squares analysis revealed an equilibrium dissociation constant of $(2.4 \pm 0.3) \times 10^{-4}$ M. Titrations with ATP performed over a temperature range from 20 to 50 °C revealed a modest decrease in the affinity as the temperature increases (Table 2), and van't Hoff analysis of the dependence of the equilibrium constant on temperature yields a binding enthalpy of -3.5 ± 1.5 kcal/mol (Figure 6B).

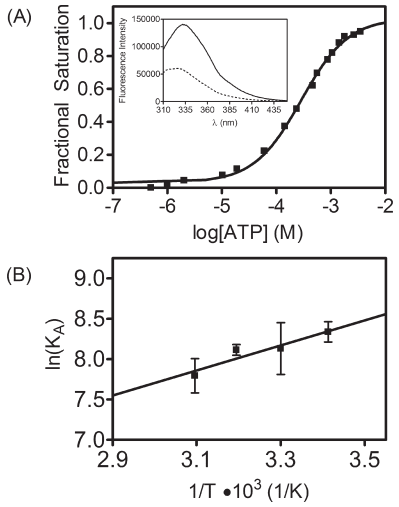

FIGURE 6: ATP binding to *Ph*BPL. (A) Normalized binding data obtained from titration of *Ph*BPL with ATP at 20 °C. The solid line represents the best fit obtained from nonlinear least-squares analysis of the data using a single-site binding model. The inset shows the fluorescence emission spectra acquired for *Ph*BPL (—) and the *Ph*BPL·ATP complex (···). (B) van't Hoff analysis of the temperature dependence of the equilibrium association constant for the *Ph*BPL−ATP interaction obtained from titrations performed from 20 to 50 °C. The solid line represents the best fit of the data to the van't Hoff equation.

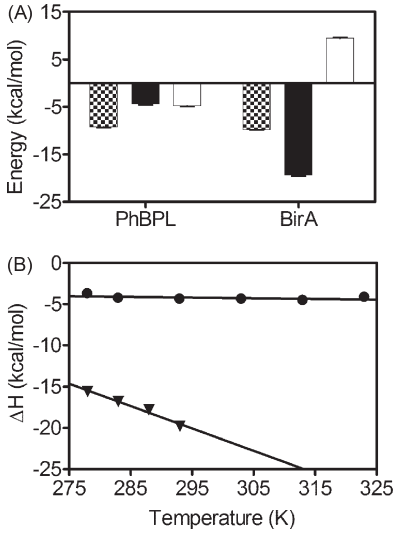

FIGURE 7: Thermodynamics of binding of biotin to *Ph*BPL and BirA are distinct. (A) The values of ΔG° (checkered) and ΔH° (black) for biotin binding to *Ph*BPL and BirA(*24*) at 20 °C were obtained from isothermal titration calorimetry. The $-T\Delta S^\circ$ (white) values were calculated using the equation $\Delta G^\circ = \Delta H - T\Delta S^\circ$. (B) Temperature dependence of biotin binding obtained either in this work from full titrations of *Ph*BPL (●) or in a previous study using the total association at partial saturation (TAPS) method for BirA (▼) (*24*). The solid lines represent the best fit of the data to the equation $\Delta C_p^\circ = d\Delta H^\circ/dT$.

Linkage between Biotin and ATP Binding. Binding of ATP and biotin to *Ph*BPL leads to enzyme-catalyzed synthesis of the intermediate, bio-5′-AMP. In the *E. coli* enzyme, no ATP binding occurs in the absence of biotin binding. By contrast, as indicated from the titrations described above, ATP does bind to the *Ph*BPL in the absence of biotin. However, it is not known if each substrate affects the binding of the second substrate to the enzyme. Thermodynamic coupling in ATP and biotin binding to

Table 2: Temperature Dependence of ATP Binding to *Ph*BPL

temperature[a] (°C)	K_D[b] (M)	$\Delta G°$[c] (kcal/mol)
20	$(2.4 \pm 0.3) \times 10^{-4}$	-4.80 ± 0.08
30	$(2.9 \pm 0.9) \times 10^{-4}$	-4.86 ± 0.02
40	$(3.0 \pm 0.2) \times 10^{-4}$	-5.00 ± 0.04
50	$(4.3 \pm 0.9) \times 10^{-4}$	-4.9 ± 0.1

[a]Measurements were performed in standard buffer [500 mM KCl, 10 mM Tris-HCl, and 2.5 mM $MgCl_2$ (pH 7.5 ± 0.2) at the indicated temperature] as described in Materials and Methods. [b]Errors correspond to the standard deviation of results obtained from at least two independent experiments. [c]The free energy, $\Delta G°$, is related to the equilibrium constant, K_D, by the expression $\Delta G° = RT \ln K_D$.

Table 3: Linkage between Biotin and ATP Binding to *Ph*BPL

ligand[a]	K_D[d] (M)	$\Delta G°$[e] (kcal/mol)
ATP	$(2.4 \pm 0.3) \times 10^{-4}$	-4.80 ± 0.08
AMPCPP	$(1.5 \pm 0.2) \times 10^{-4}$	-5.09 ± 0.08
AMPCPP/biotin[b]	$(1.4 \pm 0.3) \times 10^{-4}$	-5.1 ± 0.1
biotin	$(2.0 \pm 0.1) \times 10^{-7}$	-8.90 ± 0.04
biotin/AMPCPP[c]	$(2.6 \pm 0.3) \times 10^{-7}$	-8.74 ± 0.07

[a]Measurements were performed in standard buffer [500 mM KCl, 10 mM Tris-HCl, and 2.5 mM $MgCl_2$ (pH 7.5 ± 0.2) at 20 °C] as described in Materials and Methods. [b]α,β-Methyleneadenosine 5′-triphosphate was titrated into *Ph*BPL saturated with biotin. [c]Biotin was titrated into *Ph*BPL saturated with α,β-methyleneadenosine 5′-triphosphate. [d]Errors correspond to the standard deviation of results obtained from at least two independent experiments. [e]The free energy, $\Delta G°$, is related to the equilibrium constant, K_D, by the expression $\Delta G° = RT \ln K_D$.

*Ph*BPL was investigated by performing binding titrations with each ligand in the presence and absence of the second ligand. Fluorescence spectroscopy was used to monitor the progress of the titrations.

To prevent the chemistry that occurs upon binding of the biotin and ATP substrates, an ATP analogue was used in the linkage measurements. The analogue in which a methylene replaces the oxygen that links the α- and β-phosphates in ATP, α,β-methylene adenosine 5′-triphosphate, was used. The effect of this structural modification on the binding of the nucleotide was first investigated by measuring binding of the analogue alone to the enzyme. As observed with ATP, addition of saturating amounts of the analogue to *Ph*BPL results in quenching of the intrinsic protein fluorescence. However, in contrast to ATP binding, which results in a blue shift in the maximum of the fluorescence spectrum, binding of the analogue resulted in a red shift. Titration of *Ph*BPL with the analogue yields binding data that are described well by a simple 1:1 model with a resolved equilibrium dissociation constant of $(1.5 \pm 0.2) \times 10^{-4}$ M at 20 °C, a value similar to that measured for ATP binding under the same buffer conditions (Table 3).

The linkage between ATP and biotin binding was investigated via measurement of binding of each ligand in the presence of saturating amounts of the second ligand. Titration of the *Ph*BPL·biotin complex with the ATP analogue yields data that when subjected to nonlinear least-squares analysis using a simple binding model, reveal an equilibrium constant identical to that obtained from measurements of ATP and the ATP analogue alone (Table 3). Likewise, titration of the protein presaturated with the ATP analogue with biotin also yields an equilibrium dissociation constant for biotin binding identical to that obtained under the same conditions for biotin alone (Table 3). Thus, there is no thermodynamic linkage in biotin and ATP binding to the *P. horikoshii* enzyme.

DISCUSSION

The Dimeric Structure of PhBPL Is Independent of Ligation State. In all *Ph*BPL structures determined by X-ray crystallography, the protein is dimeric (*9*). In this work, equilibrium analytical ultracentrifugation measurements performed on the apoenzyme and its complexes with biotin and bio-5′-AMP all yield molecular masses for the protein consistent with a dimer. Thus, regardless of ligation state, the *P. horikoshii* enzyme is a dimer. Furthermore, the lack of evidence of any monomer in the sedimentation equilibrium measurements is consistent with a very stable dimer interface.

The oligomerization properties of monofunctional biotin protein ligases are not conserved. High-resolution structures of other monofunctional biotin protein ligases are available, including those from *Mycobacterium tuberculosis* and *Aquifex aeolicus* (*10*). Although at the monomer level these two proteins are structurally similar to the *P. horkoshii* enzyme, the oligomeric state can be either monomeric or dimeric. Moreover, in the dimeric enzymes observed in the crystal structures, the surface utilized for dimerization is not conserved. The *P. horikoshii* enzyme dimerizes using the N-terminal β-strand of the large sheet that characterizes the core of the enzyme active site domain (Figure 2). By contrast, in the *M. tuberculosis* dimer, the C-terminal SH3-like domain is utilized in dimerization (Protein Data Bank entry 2CGH). Moreover, size exclusion chromatography measurements indicate that this dimer is not stable (*22*).

Formation of the homodimer by the bifunctional *E. coli* biotin protein ligase is coupled to bio-5′-AMP binding (*14*). Kinetic measurements of bio-5′-AMP synthesis by the *E. coli* monomer indicate that substrate binding in adenylate synthesis occurs via an obligatorily ordered process in which biotin binding precedes ATP binding (*13*). Consequently, the activation of dimerization by bio-5′-AMP binding renders dimerization and, therefore, transcription regulation sensitive to biotin concentration (Figure 1A). In addition, the surface used for BirA homodimerization is identical to that used for heterodimerization with apoBCCP (Figure 2). This mutually exclusive nature of the homo- and heterodimerization provides a mechanism for regulation of the functional switch between the post-translational modification enzyme and the transcriptional repressor (*16*, *17*). By contrast, the oligomerization properties of the monofunctional ligases do not appear to serve any regulatory function.

Thermodynamic Parameters Governing Biotin and ATP Binding to PhBPL. The thermodynamics of the binding of biotin to *Ph*BPL indicate relatively modest affinity. The equilibrium dissociation constant governing biotin binding at 20 °C is approximately 200 nM. Additionally, the relatively modest temperature dependence of binding suggests that even at the optimal growth temperature for *P. horikoshii* of 98 °C the equilibrium dissociation constant will be approximately 1.6×10^{-6} M. In *E. coli*, the total biotin concentration is estimated to be in the nanomolar concentration range. Assuming similar intracellular biotin concentrations in *P. horikoshii* and that the K_M for biotin binding is equal to the K_D, we find the substrate concentration is considerably lower than the K_M. In addition to the Gibbs free energy of biotin binding, the enthalpy of the interaction is modest (−4.4 kcal/mol). The result of this modest enthalpy is that even at the optimal growth temperature of 98 °C the protein still has considerable affinity for the substrate. Biotin binding to the *E. coli* enzyme is characterized by an enthalpy of approximately

−20 kcal/mol at 20 °C (Figure 7A) (*23*). Nonetheless, at 37 °C, the equilibrium dissociation constant governing biotin binding to the *E. coli* ligase is 1.3×10^{-7} M, a value that is 10-fold lower than that predicted for the *P. horikoshii* enzyme at its optimal growth temperature. Finally, while biotin binding to *Ph*BPL is characterized by a heat capacity change that is, within error, zero, biotin binding to the *E. coli* enzyme is characterized by a substantial heat capacity change of approximately −0.2 to −0.3 kcal mol^{-1} K^{-1} (*24*, *25*).

The thermodynamics of biotin binding to two other monofunctional biotin ligases have been determined. Consistent with results for the *Ph*BPL described in this work, biotin binding the *A. aeolicus* and *M. tuberculosis* enzymes is weaker than for the *E. coli* enzyme (*10*, *22*). The difference between the monofunctional and bifunctional enzymes potentially facilitates the role of the bifunctional enzyme in regulating biotin biosynthesis, with the greater sensitivity of the *E. coli* enzyme to biotin concentration enabling feedback of increased biotin concentration to transcription repression at the biotin biosynthetic operon.

In contrast to the bifunctional *E. coli* enzyme, to which ATP binding cannot be detected in the absence of biotin binding, the nucleotide substrate binds to the *P. horikoshii* enzyme on its own. Measurements of the affinity indicate a K_D in the concentration range of 200−400 μM in the temperature range of 20−50 °C. Moreover, the binding enthalpy is modest. Consequently, the affinity at the optimal growth temperature of 98 °C is expected to be similar to the values reported in this work. The independence of ATP and biotin binding to the *Ph*BPL is consistent with observations made on the monofunctional *A. aeolicus* BPL. Both of these enzymes share several structural features with the *E. coli* enzyme, including a biotin binding loop and an adenylate binding loop. In the *E. coli* enzyme, this latter loop is disordered in both the apoenzyme structure and the biotin-bound structure and is ordered only in the complex of the protein bound to the adenylate analogue, biotinol-5′-AMP. By contrast, the loop is ordered in the structures of the unliganded forms of both monofunctional enzymes (*9*, *10*). It has been proposed that this ordering renders the nucleotide binding site "preorganized" in the monofunctional enzyme, thereby allowing nucleotide binding that is independent of biotin.

No coupling is observed in ATP and biotin binding to *Ph*BPL. The affinities for biotin and the ATP analogue, α,β-methyleneadenosine 5′-triphosphate, are identical regardless of the occupancy of the site by the second ligand. This result is somewhat surprising in the context of the structural data available for the enzyme. In the absence of any ligand, the biotin binding loop of the enzyme is disordered. Structures of the biotin and ADP-bound protein indicate ordering of the loop. One might anticipate that the preordering that is a consequence of binding of one substrate would facilitate binding of the second substrate.

Previously published results combined with the results described in this work suggest that both coupling between biotin and ATP binding and the order of substrate binding are correlated with ligase functionality. The bifunctional *E. coli* enzyme does not bind ATP in the absence of biotin (ref *13* and recent direct binding studies performed by K.G.D.). By contrast, both the *P. horikoshii* and *A. aeolicus* enzymes bind the nucleotide in the absence of biotin. In addition, the micromolar equilibrium dissociation constants for ATP binding by the monofunctional ligases are significantly lower than the K_M for ATP in *E. coli* BPL-catalyzed bio-5′-AMP synthesis of approximately 3 mM (*13*). Linkage in binding of the two substrates has been measured for the *A. aeolicus* enzyme. However, these measurements are inconclusive because while they indicate no coupling when ATP binding is measured in the presence of saturating biotin, a coupling free energy of approximately −1.0 kcal/mol was estimated from measurements of biotin binding in the presence and absence of ATP (*10*). The discrepancy may result from the fact that, to avoid chemistry, these binding measurements were performed in the absence of Mg^{2+}, an essential cofactor in catalysis of bio-5′-AMP synthesis that is included in all buffers used in the measurements reported in this work (*1*). These authors concluded that, consistent with the *P. horikoshii* enzyme, addition of the substrate to the *A. aeolicus* enzyme occurs via a random mechanism. By contrast, the *E. coli* enzyme functions in an obligatorily ordered mechanism, which renders biotin concentration a trigger for accumulation of the activated BirA·bio-5′-AMP species (Figure 1).

Monofunctional and bifunctional microbial biotin ligases have evolved distinct mechanisms of substrate binding and self-association. The monofunctional ligases are either constitutive monomers or dimers. Moreover, in these enzymes, dimerization is independent of substrate or intermediate binding. By contrast, the bifunctional *E. coli* ligase is a conditional homodimer that depends on the formation of the adenylated intermediate and is utilized solely for the transcriptional regulatory function. Substrate binding mechanisms are also distinct for the two classes of BPLs, with the monofunctional ligases exhibiting ATP binding in the absence of biotin and a random mechanism of ATP and biotin binding. This contrasts with BirA, which requires biotin binding prior to nucleotide binding. Superficially, the two classes of ligases are similar in both primary sequence and tertiary structure. Previous studies suggest that the distinct dimerization properties of the bifunctional enzyme result from evolution of the sequences of surface loops on the protein (*26*, *27*). The distinct substrate binding properties of the monofunctional and bifunctional enzymes may also be related to properties of the adenylate binding loop. While the loop in BirA is disordered in the absence of ligand, in the *P. horikoshii* and *A. aeolicus* enzymes it is ordered. This ordered loop conformation may confer on the monofunctional ligases both the ability to bind nucleotide in the absence of biotin and the resulting random mechanism of substrate binding.

ACKNOWLEDGMENT

We thank the RIKEN group for supplying the plasmid used for overexpression of *Ph*BPL.

REFERENCES

1. Lane, M. D., Rominger, K. L., Young, D. L., and Lynen, F. (1964) The enzymatic synthesis of holotranscarboxylase from apotranscarboxylase and (+)-biotin. *J. Biol. Chem. 239*, 2865–2871.
2. Rodionov, D. A., Mironov, A. A., and Gelfand, M. S. (2002) Conservation of the biotin regulon and the BirA regulatory signal in Eubacteria and Archaea. *Genome Res. 12*, 1507–1516.
3. Rodionov, D. A., and Gelfand, M. S. (2006) Computational identification of BioR, a transcriptional regulator of biotin metabolism in Alphaproteobacteria, and of its binding signal. *FEMS Microbiol. Lett. 255*, 102–107.
4. Barker, D. F., and Campbell, A. M. (1981) The birA gene of *Escherichia coli* encodes a biotin holoenzyme synthetase. *J. Mol. Biol. 146*, 451–467.
5. Barker, D. F., and Campbell, A. M. (1981) Genetic and biochemical characterization of the birA gene and its product: Evidence for a direct role of biotin holoenzyme synthetase in repression of the biotin operon in *Escherichia coli*. *J. Mol. Biol. 146*, 469–492.

6. Wilson, K. P., Shewchuk, L. M., Brennan, R. G., Otsuka, A. J., and Matthews, B. W. (1992) *Escherichia coli* biotin holoenzyme ynthetase/bio repressor crystal structure delineates the biotin- and DNA-binding domains. *Proc. Natl. Acad. Sci. U.S.A. 89*, 9257–9261.
7. Weaver, L. H., Kwon, K., Beckett, D., and Matthews, B. W. (2001) Corepressor-induced organization and assembly of the biotin repressor: A model for allosteric activation of a transcriptional regulator. *Proc. Natl. Acad. Sci. U.S.A. 98*, 6045–6050.
8. Wood, Z., Weaver, L. H., Brown, P. H., Beckett, D., and Matthews, B. W. (2006) Co-repressor induced order and biotin repressor dimerization: A case for divergent followed by convergent evolution. *J. Mol. Biol. 357*, 509–523.
9. Bagautdinov, B., Kuroishi, C., Sugahara, M., and Kunishima, N. (2005) Crystal structures of biotin protein ligase from *Pyrococcus horikoshii* OT3 and its complexes: Structural basis of biotin activation. *J. Mol. Biol. 353*, 322–333.
10. Tron, C. M., McNae, I. W., Nutley, M., Clarke, D. J., Cooper, A., Walkinshaw, M. D., Baxter, R. L., and Campopiano, D. J. (2009) Structural and functional studies of the biotin protein ligase from *Aquifex aeolicus* reveal a critical role for a conserved residue in target specificity. *J. Mol. Biol. 387*, 129–146.
11. Abbott, J., and Beckett, D. (1993) Cooperative binding of the *Escherichia coli* repressor of biotin biosynthesis to the biotin operator sequence. *Biochemistry 32*, 9649–9656.
12. Streaker, E. D., and Beckett, D. (2003) Coupling of protein assembly and DNA binding:biotin repressor dimerization preceeds biotin operator binding. *J. Mol. Biol. 325*, 937–948.
13. Xu, Y., and Beckett, D. (1994) Kinetics of biotinyl-5′-adenylate synthesis catalyzed by the *Escherichia coli* repressor of biotin biosynthesis and the stability of the enzyme-product complex. *Biochemistry 33*, 7354–7360.
14. Eisenstein, E., and Beckett, D. (1999) Dimerization of the *Escherichia coli* biotin repressor:corepressor function in protein assembly. *Biochemistry 38*, 13077–13084.
15. Weaver, L. H., Kwon, K., Beckett, D., and Matthews, B. W. (2001) Competing protein:protein interactions are proposed to control the biological switch of the *E. coli* biotin repressor. *Protein Sci. 10*, 2618–2622.
16. Streaker, E. D., and Beckett, D. (2006) The biotin regulatory system: Kinetic control of a transcriptional switch. *Biochemistry 45*, 6417–6425.
17. Zhao, H., and Beckett, D. (2008) Kinetic partitioning between alternative protein-protein interactions controls a transcriptional switch. *J. Mol. Biol. 380*, 223–236.
18. Prakash, O., and Eisenberg, M. A. (1979) Biotinyl 5′-adenylate: Corepressor role in the regulation of the biotin genes of *Escherichia coli* K-12. *Proc. Natl. Acad. Sci. U.S.A. 76*, 5592–5595.
19. Gill, S. C., and von Hippel, P. H. (1989) Calculation of protein extinction coefficients from amino acid sequence data. *Anal. Biochem. 182*, 319–326.
20. Johnson, M. L., Correia, J. J., Yphantis, D. A., and Halvorson, H. R. (1981) Analysis of data from the analytical ultracentrifuge by nonlinear least-squares techniques. *Biophys. J. 36*, 575–588.
21. Gonzalez, J. M., Masuchi, Y., Robb, F. T., Ammerman, J. W., Maeder, D. L., Yanagibayashi, M., Tamaoka, J., and Kato, C. (1998) *Pyrococcus horikoshii* sp. nov., a hyperthermophilic archaeon isolated from a hydrothermal vent at the Okinawa Trough. *Extremophiles 2*, 123–130.
22. Purushothaman, S., Gupta, G., Srivastava, R., Ramu, V. G., and Surolia, A. (2008) Ligand specificity of group I biotin protein ligase of *Mycobacterium tuberculosis*. *PLoS One 3*, e2320.
23. Brown, P. H., and Beckett, D. (2005) Use of binding enthalpy to drive an allosteric transition. *Biochemistry 44*, 3112–3121.
24. Naganathan, S., and Beckett, D. (2007) Nucleation of an allosteric response via ligand-induced loop folding. *J. Mol. Biol. 373*, 96–111.
25. Brown, P., and Beckett, D. (2005) Use of binding enthalpy to drive an allosteric response. *Biochemistry 44*, 3112–3121.
26. Kwon, K., Streaker, E. D., Ruparelia, S., and Beckett, D. (2000) Multiple disordered loops function in corepressor-induced dimerization of the biotin repressor. *J. Mol. Biol. 304*, 821–833.
27. Zhao, H., Naganathan, S., and Beckett, D. (2009) Thermodynamic and structural investigation of bispecificity in protein-protein interactions. *J. Mol. Biol. 389*, 336–348.
28. Koradi, R., Billeter, M., and Wuthrich, K. (1996) MOLMOL: A program for display and analysis of macromolecular structures. *J. Mol. Graphics 14*, 29–32, 51−55.